

# Study of Heat Source Calibration and Modelling for Laser Welding Process

Changrong Chen<sup>1,2,#</sup>, Yueh-Jaw Lin<sup>2</sup>, Hengan Ou<sup>3</sup>, and Yan Wang<sup>4</sup>

<sup>1</sup> School of Mechanical and Automotive Engineering, Fujian University of Technology, No 3 Xueyuan Road, Fuzhou, 350-118, China

<sup>2</sup> Faculty of Science and Engineering, University of Nottingham Ningbo China, 199, Taikang East Road, Ningbo, 315-100, China

<sup>3</sup> Department of Mechanical, Materials and Manufacturing Engineering, University of Nottingham, University Park, Nottingham, NG7 2RD, United Kingdom

<sup>4</sup> School of Computing, Engineering and Mathematics, University of Brighton, Mithras House, Lewes Road, Brighton, BN2 4AT, United Kingdom

# Corresponding Author / E-mail: changrong.chen@fjut.edu.cn, TEL: +86-591-22863543

ORCID: 0000-0002-8709-5721

KEYWORDS: Heat source model, Laser welding, Finite element modelling, Mathematical modelling

*Heat source model is an important part when carrying out simulations of welding processes. The calibration process involves a great amount of numerical simulations or theoretical deductions with many simplifications. In this paper, an interaction finite element and optimization algorithm package is programmed to automatically calibrate heat source models. The results are then used to establish mathematical relationships between parameters of heat source and welding process variables. The models show that the absorption efficiency and depth of heat source are exponential functions of depth of focus and laser power, respectively while radius of heat source is determined by depth of focus quadratically.*

Manuscript received: April 11, 2017 / Revised: May 30, 2018 / Accepted: June 6, 2018

## NOMENCLATURE

$c$  = specific heat capacity  
 $D_f$  = depth of defocus of a heat  
 $f$  = frequency of laser pulse  
 $H$  = depth of a heat source  
 $I$  = current for laser generation  
 $k$  = thermal conductivity  
 $q$  = heat flux density of laser on workpiece  
 $\dot{q}$  = rate of heat distributed in workpiece  
 $Q$  = laser power  
 $r_0$  = radius of a heat source  
 $r$  = radial distance of a point from the symmetric heat source axis  
 $t$  = time  
 $T$  = temperature  
 $v$  = scanning speed of laser beam  
 $\rho$  = density  
 $\eta$  = energy absorption efficiency

## 1. Introduction

Heat input model is one important part when carrying out welding relevant simulations. The interaction of a heat source (arc, electron beam or laser beam) with a weld pool remains a complex physical phenomenon due to the arc digging and stirring, thus still cannot be modelled rigorously. Welding analysts have been devoted much of their effort to developing different heat source models that could describe the shape of weld and the temperature field in workpieces.

It is significant to accurately define the parameters associated with the mathematical description of the heat source because all simulations in Computational Welding Mechanics (CWM) consider only thermo-mechanical phenomena in the weld and incorporate all the physics of the welding processes into empirical heat input models.<sup>1-3</sup> Thus the heat source model must be calibrated so that the simulations yield results closely correlating with the experimental data. After calibration, the parameters of heat source can be used for transient analysis.<sup>3</sup>

The calibration is usually achieved by carrying out an inverse modelling (or optimization), either numerically or analytically. Temperature-related weld characteristics such as temperature history and weld profiles are frequently utilized for the estimation of unknown parameters.<sup>4,5</sup> The calibration process using numerical methods requires

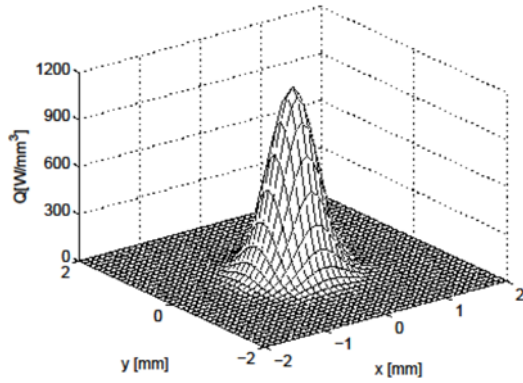


Fig. 1 Heat source power distribution at the top surface

iterative changing of parameters and checking of divergence in weld characteristics.<sup>3</sup> Therefore, the process is usually condemned for being time consuming and labour intensive. Analytical solutions, on the other hand, is capable of calibrating heat source models with a dramatic reduction in computation and interaction. However, it requires sound knowledge in physics and theoretical deduction. Also, the theory is usually obtained with some simplifications.<sup>6</sup> Moreover, proportional expressions are commonly used to establish heat source models. The linear relationships are susceptible to environmental noise, which would cause significant divergence in weld output.<sup>5</sup>

To overcome the problems, an automatic interaction program is proposed in this paper based on commercial finite element modelling (FEM) and optimization packages. The automatic calibration process enables great saving of heavy labour. Furthermore, this method does not require much knowledge of theoretical heat transfer analysis. The calibration results are then used to establish mathematical models behind the source model parameters and laser welding process variables which could be used for simulations under other welding process conditions. The physics about the effect of welding variables on heat source parameters are explained, followed by the discussion of feasibility of these mathematical models.

## 2. Heat Source Model for Laser Welding

The proposed heat input models in literature range from point source model, disc model, Gaussian heat source model to ellipsoidal power density distribution.<sup>2,4,7,8</sup> For laser and electron beam welding processes which have a comparatively concentrated energy distribution and deep penetration, a conical heat source with uniform heat flux as some Gaussian distribution may yield more accurate results.<sup>2,7,8</sup> The heat flux with a Gaussian distribution can be represented as

$$q(r) = q(0)e^{-cr^2} \quad (1)$$

where  $q(0)$  is the maximum heat flux,  $c$  the concentration coefficient and  $r$  the radial distance of a point from the symmetric heat source axis.

The major problem then becomes the determination of heat flux distribution along the thickness. Analyses suggest that the laser beam power decreases with increasing penetration depth.<sup>7,9</sup> Different shapes

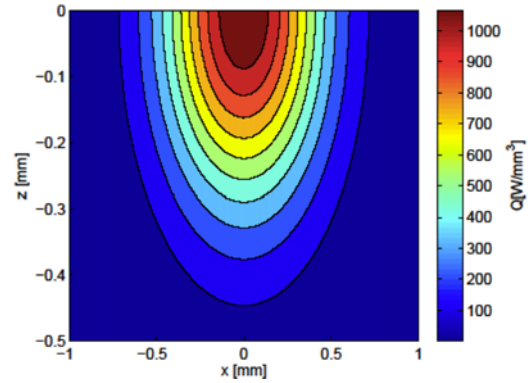


Fig. 2 Heat source power distribution in cross section

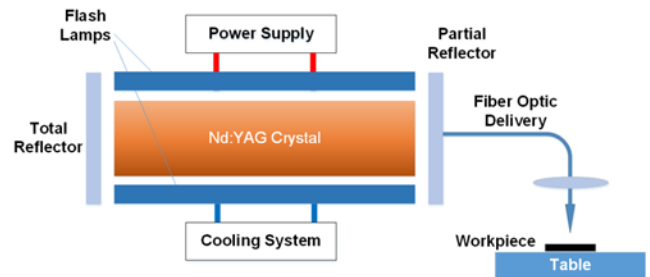


Fig. 3 Schematic representation of the pulsed Nd:YAG laser welding system

along the depth are considered in laser beam heat source models to account for this effect. In this study, Goldak ellipsoidal power density distribution is considered for laser welding modelling:

$$q(r) = \frac{6\sqrt{3}\eta Q}{\pi\sqrt{\pi}r_0^2 H} e^{\left(-\frac{3r^2}{r_0^2} - \frac{3z^2}{H^2}\right)} \quad (2)$$

where  $\eta$  is the energy absorption efficiency,  $Q$  the laser power,  $r_0$  the radius of the heat source, and  $H$  the depth of the heat source, respectively. Figs. 1 and 2 illustrate the power distributions at the top surface ( $z = 0$ ) and in the cross section ( $y = 0$ ) as a Goldak heat source is focused on the material surface, respectively. From the figures, one can find that the power is normally distributed along distance from the heat source centre.

## 3. Calibration Process

A pulsed Nd:YAG laser welder of 300W power (WF300, HAN'S) is utilized as a machining tool in this study. The configuration of the pulsed Nd:YAG laser beam welding system is illustrated in Fig. 3. The energy per pulse generated by the laser system is correlated with current, as shown in Fig. 4.

The calibration of heat source is performed by comparing fusion zone temperature contours from simulation with the corresponding weld macrographs. Experimental tests were carried out to remelt workpieces with dimensions of  $100 \times 100 \times 7.5$  mm, made of ASSAB 8407 supreme hot work steel, under process conditions listed in Table 1. Weld profiles were then prepared by sectioning the weld trajectory in

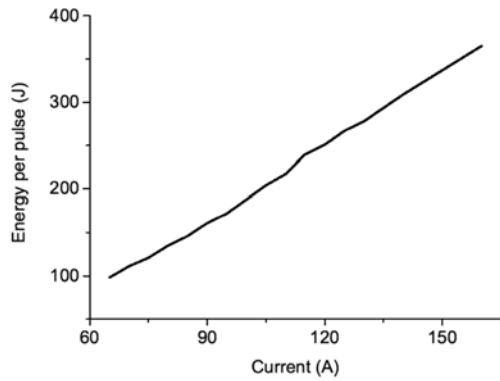


Fig. 4 Relationship between energy per pulse and current in Han's laser system

Table 1 Process parameters used for heat source calibration of laser welding

Weld No.	Current ( $I$ , A)	Depth of Defocus ( $D_f$ , mm)	Scanning Speed ( $v$ , mm/s)	Frequency ( $f$ , Hz)
1	80	-2	0.9	10
2	95	-3	0.6	7
3	110	-4	0.3	4
4	125	-1	0.3	10

transverse direction. While in the simulation, weld macrographs were defined by the contour of material melting temperature, i.e., 1447°C.

The governing differential equation of heat conduction in the workpiece when being laser surfaced is given as follows:

$$\nabla \cdot (k \nabla T) + \dot{q} = \rho c \frac{\partial T}{\partial t} \quad (3)$$

where  $T$  is temperature,  $t$  is time,  $k$  is the thermal conductivity,  $c$  is the specific heat capacity,  $\rho$  is the density and  $\dot{q}$  is the rate of heat distributed in the workpiece.

An interaction between ABAQUS<sup>®</sup> and MATLAB<sup>®</sup> was built for the calibration process, as the flow chart indicated in Fig. 5. The entire calibration process is conducted within the MATLAB<sup>®</sup> programming environment. A sample FEM script is firstly established using Python programming tool. The unknown parameters in this file and the user subroutine are then modified by file operation in MATLAB<sup>®</sup>, followed by the call of ABAQUS<sup>®</sup> for FEA execution. The results of temperature field obtained from each FEM calculation are exported to sketch the simulated weld macrograph which is compared with experimental data to optimize the unknown parameters until the divergence is minimized.

Fig. 6 shows the analysis model and moving direction of the pulsed laser beam. Due to geometric symmetry, only half the plate was modelled to reduce computation effort. A fine mesh was used for areas in contact with the laser beam since they experienced a complicated thermal sequence of momentary heating and cooling. A subroutine was created to define the shape and motion of laser heat source. And the laser pulse was simulated with fixed average beam power of the welding condition.

Boundary conditions for the simulation include heat input condition of the laser beam, convection and radiation of surfaces exposed to the air. Thermal properties in this simulation were also considered

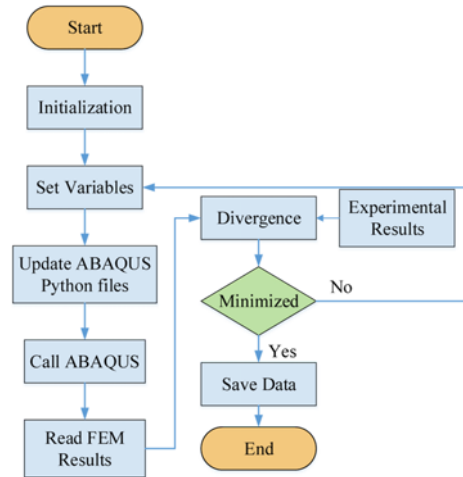


Fig. 5 Heat source calibration flow chart

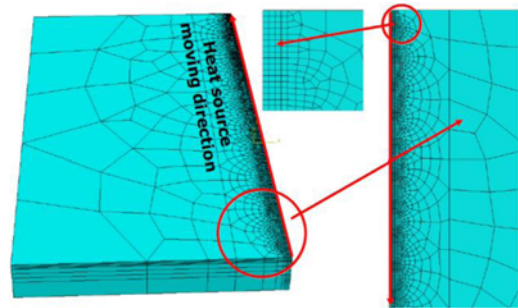


Fig. 6 Half model of the plate for heat source calibration

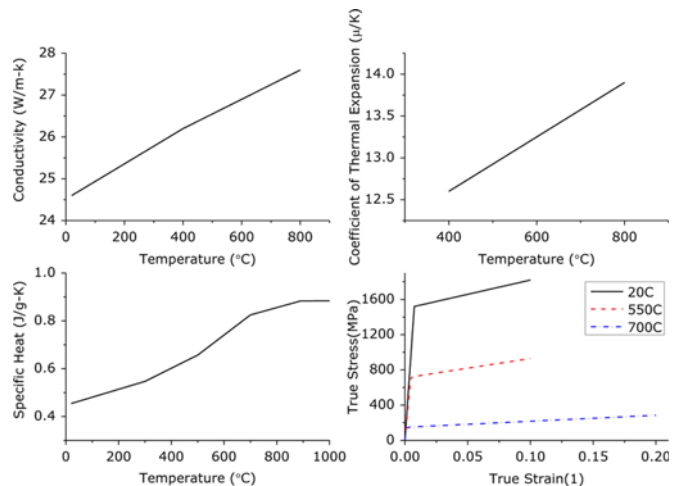


Fig. 7 Material properties of ASSAB 8407S mould steel

temperature-dependent, as summarized in Fig. 7. Some properties of high temperatures in literature were used.<sup>4,10,11</sup>

#### 4. Results and Discussion

Table 2 denotes the results of heat source model calibration. An obvious comparison can be made through the weld profiles obtained by

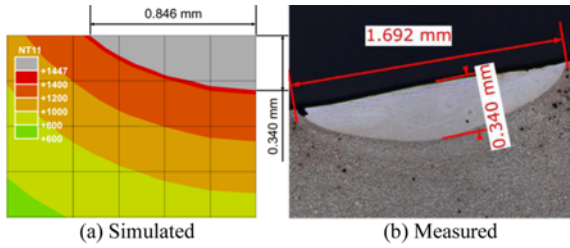


Fig. 8 Comparison of FEM calculated and experimental weld macrographs for parameters (80 A, -2 mm, 0.9 mm/s, 10 Hz)

Table 2 Calibration results of laser heat source models

Weld No.	Measured weld width (mm)	Measured weld depth (mm)	Simulated weld width (mm)	Simulated weld depth (mm)
1	1.693	0.340	1.692	0.340
2	1.803	0.331	1.803	0.331
3	1.932	0.278	1.932	0.277
4	1.884	0.688	1.883	0.688

Table 3 Parameters calibrated for laser heat source models

Weld No.	$I$	$D_f$	$v$	$f$	$\eta$	$r_0$ (mm)	$H$ (mm)
1	80	-2	0.9	10	0.129	1.879	0.193
2	95	-3	0.6	7	0.149	2.143	0.188
3	110	-4	0.3	4	0.198	2.962	0.149
4	125	-1	0.3	10	0.094	1.697	0.826

Table 4 Pearson correlation of heat source model variables

	$D_f$	$Q$	$\eta$	$r_0$	$H$
$D_f$	1.000	0.903	-0.987*	-0.938	0.808
$Q$	0.903	1.000	-0.891	-0.755	0.981*
$\eta$	-0.987*	-0.891	1.000	0.969*	-0.786
$r_0$	-0.938	-0.755	0.969*	1.000	-0.613
$H$	0.808	0.981*	-0.786	-0.613	1.000

\*: Correlation is significant at the 0.05 level (2-tailed).

the simulation and experimentation, as shown in Fig. 8. From the figure, we can observe that the divergence between numerical and experimental weld profiles could be ignored. Therefore, the parameters of heat source model are identified for these process conditions, as depicted in Table 3. According to common practice, it is available for establishing mathematical relationships between these parameters and welding process conditions.

A correlation matrix was proposed using IBM SPSS® Statistics 22, as shown in Table 4, to investigate the correlations among these variables. From Table 4, one can find that the laser absorption efficiency is significantly correlated with depth of defocus while the depth of heat source is strongly relevant to laser power. The radius of heat source is not significantly related to depth of heat source or laser power. But it is probably connected with the absorption efficiency, thereby being affected by depth of focus as well.

On the other hand, it is also telling from Table 4 that all three heat source parameters,  $\eta$ ,  $r_0$  and  $H$ , are not dependent on process variables: scanning speed and frequency of laser pulse. Both two variables are

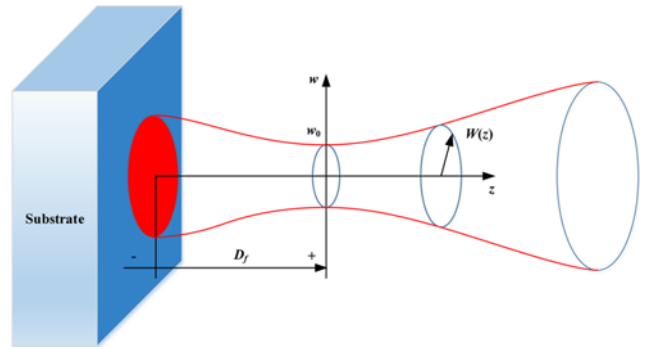


Fig. 9 Facula of Gaussian beam ( $w_0$ , waist of Gaussian beam;  $w(z)$ , radius of beam at  $z$  from focus position;  $D_f$ , the distance of beam waist outside (negative for inside) the substrate)

Table 5 Model summary of curve estimations for heat source parameters

Heat source parameter	Equation	R Square
$\eta$	$\eta = 0.0755e^{-0.239D_f}$ (4)	0.981
$r_0$	$r_0 = 1.95 + 0.39D_f + 0.159D_f^2$ (5)	0.988
$H$	$H = 0.056e^{0.001P_a}$ (6)	0.987

significant factors influencing the final state of laser welding, e.g., microstructure, weld profile and residual stresses, etc. However, their effects on the heat source model can be negligible, according to the correlation study. The principal reason is that the heat source model is crucially determined by the mode of laser beam ( $TEM_{00}$  here) and laser-substrate interaction, other than the moving speed and frequency of laser. Fig. 9 depicts a typical profile of Gaussian beam for the utilized laser. The spot size of laser beam  $w(z)$  is related to distance from focus  $z$  in a hyperbolic manner.<sup>12</sup> Therefore, the radius of heat source model  $r_0$  should also be decided by depth of defocus. The efficiency and depth of heat source are mainly determined by the laser-material interaction, thereby reasonably being correlated to depth of defocus and laser power, respectively. As a result, the parameters of heat source model are independently defined in simulation.

The mathematical models of three parameters of heat source model were constructed using the curve estimation in IBM SPSS® Statistics 22 environment. For simplicity, the parameters of heat source model were assumed to be dependent on the significant variable only. Table 5 summarizes the estimated models for three heat source parameters. From Table 5, we can find that all these three parameters are not linearly determined by welding process parameters. Specifically, the absorption efficiency of laser beam and depth of heat source are exponentially related to depth of focus and laser power, respectively while the radius of heat source is more relevant with depth of focus in quadratic manner. Figs. 10-12 depict the variations of three heat source model parameters in terms of depth of defocus and laser power, respectively. From the figures, one can tell that the absorption efficiency and heat source radius decrease as the laser focus moves outward the substrate material, whereas the heat source depth increases as laser power rises.

The relationships of heat source model parameters correlated to the

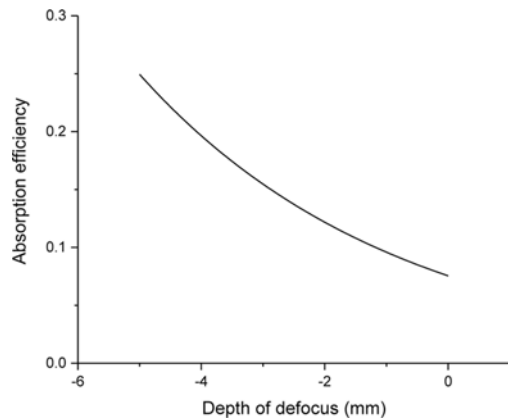


Fig. 10 Variation of absorption efficiency of laser to material with defocus depth

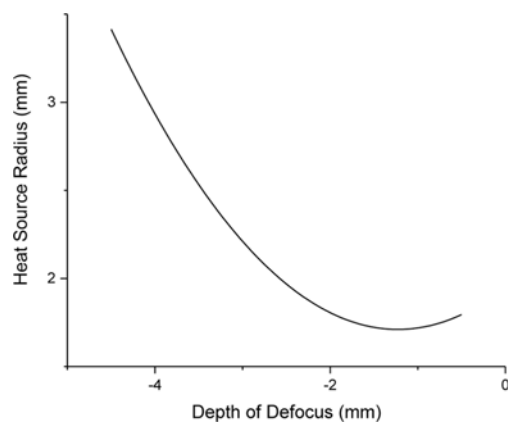


Fig. 11 Variation of heat source radius with defocus depth

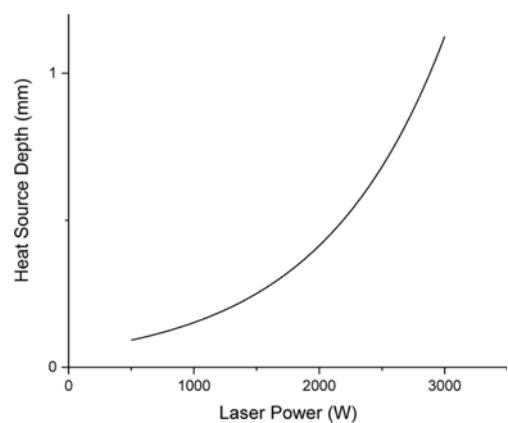


Fig. 12 Variation of heat source depth with laser power

process variables can be explained as follows. The laser achieves maximum power density at the focus position (or beam waist) and decreases with defocusing. The deeper the beam focus underneath the substrate, the more power targeted upon the material. The greater power density potential then leads to better absorption of laser energy. The radius of heat source is affected by the depth of defocus due to the characteristic of laser beam, as explained previously. And as the power increases, thermal gradient between the surface and the bottom of the

substrate gets more dramatic, more material will be heated up by the laser energy, thereby leading to a greater depth of heat source.

The *R*-square values listed in Table 5 indicate that three mathematical models achieve goodness-of-fit to the experimental data. The applicability of three models depends on the way process variables influence response parameters. The depth of defocus continuously affects power density targeting at the material, thereby influencing the absorption efficiency likewise. As the laser focus departs from the surface, less laser energy is absorbed by the substrate. Therefore, the relationship between absorption efficiency and depth of defocus should also be functioning for the positive defocus depth as well. However, for the radius of heat source, the expression is not identical to the hyperbolic relation of Gaussian beam and not symmetric about zero depth of defocus. The extension of this correlation to positive depth of defocus should be further investigated. The effect of laser power on the heat source is continuous, then the expression for the depth of heat source should be working for the entire domain as well.

Although the experimental data were obtained from conduction mode laser welding, the relationships established should also be flexible for keyhole laser welding. It is believed that the mode of laser welding is mostly determined by the beam power and its focus position relative to the work piece. When positively defocused (above the surface) with low power density, the laser beam heats up the material in conduction way. As it focuses below the surface and with sufficient power density, the beam will evaporate the material and form a hole in the melt pool.<sup>13</sup> Therefore, the major difference between conduction and keyhole welding is the power density applied to the welding area.<sup>14</sup> As the depth of defocus is negative (below the surface) in this work, welding mode will shift to keyhole state with increase of power. Thus, the heat source model calibrated should be feasible for both two modes.

## 5. Conclusions

In this study, heat source models for laser welding process were automatically calibrated by an interaction program between FEM and optimization package. The results were then used to determine the relationships between heat source parameters and welding process conditions. Based on these results, the following conclusions can be drawn.

- The developed interaction is capable of calibrating heat source parameters accurately.
- Absorption efficiency and radius of heat source are closely related to depth of focus, while depth of heat source is mainly affected by laser power.
- The absorption efficiency and depth of heat source are exponential functions of depth of focus and laser power, respectively. However, radius of heat source is quadratically determined by depth of focus.

## ACKNOWLEDGEMENT

The authors would like to appreciate the support from the National Natural Science Foundation of China (Grant No. 51575110) and the Ministry of Industry and Information Technology (2016-755-63). They

also wish to acknowledge the support from Ningbo Municipal Bureau of Science and Technology (Project ID 2011B81006).

## REFERENCES

1. Lindgren, L.-E., "Finite Element Modeling and Simulation of Welding Part 1: Increased Complexity," *Journal of Thermal Stresses*, Vol. 24, No. 2, pp. 141-192, 2001.
2. Lindgren, L.-E., "Computational Welding Mechanics: Thermomechanical and Microstructural Simulations," Woodhead Publishing, 2007.
3. Deshpande, A., Tanner, D., Sun, W., Hyde, T., and McCartney, G., "Combined Butt Joint Welding and Post Weld Heat Treatment Simulation Using Sysweld and Abaqus," *Proceedings of the Institution of Mechanical Engineers, Part L: Journal of Materials: Design and Applications*, Vol. 225, No. 1, pp. 1-10, 2011.
4. Klobčar, D., Tušek, J., and Taljat, B., "Finite Element Modeling of GTA Weld Surfacing Applied to Hot-Work Tooling," *Computational Materials Science*, Vol. 31, Nos. 3-4, pp. 368-378, 2004.
5. Kim, K., Lee, J., and Cho, H., "Analysis of Pulsed Nd: YAG Laser Welding of AISI 304 Steel," *Journal of Mechanical Science and Technology*, Vol. 24, No. 11, pp. 2253-2259, 2010.
6. Karkhin, V., Pittner, A., Schwenk, C., and Rethmeier, M., "Simulation of Inverse Heat Conduction Problems in Fusion Welding with Extended Analytical Heat Source Models," *Frontiers of Materials Science*, Vol. 5, No. 2, pp. 119-125, 2011.
7. Goldak, J. A. and Akhlaghi, M., "Computational Welding Mechanics," Springer Science & Business Media, 2006.
8. Lindgren, L.-E., "Numerical Modelling of Welding," *Computer Methods in Applied Mechanics and Engineering*, Vol. 195, Nos. 48-49, pp. 6710-6736, 2006.
9. Lindgren, L.-E., Häggblad, H.-A., McDill, J., and Oddy, A. S., "Automatic Remeshing for Three-Dimensional Finite Element Simulation of Welding," *Computer Methods in Applied Mechanics and Engineering*, Vol. 147, Nos. 3-4, pp. 401-409, 1997.
10. Klobčar, D., Tušek, J., and Taljat, B., "Thermal Fatigue of Materials for Die-Casting Tooling," *Materials Science and Engineering: A*, Vol. 472, Nos. 1-2, pp. 198-207, 2008.
11. Klobčar, D. and Tušek, J., "Thermal Stresses in Aluminium Alloy Die Casting Dies," *Computational Materials Science*, Vol. 43, No. 4, pp. 1147-1154, 2008.
12. Kannatey-Asibu Jr, E., "Principles of Laser Materials Processing," John Wiley & Sons, 2009.
13. Majumdar, J. D. and Manna, I., "Laser-Assisted Fabrication of Materials," Springer Science & Business Media, 2012.
14. Katayama, S., "Handbook of Laser Welding Technologies," Elsevier, 2013.